CORE
Metadata, citation and similar papers at core.ac.uk
Provided by IntechOpen

We are IntechOpen, the world's leading publisher of Open Access books Built by scientists, for scientists

4,800
Open access books available

122,000
International authors and editors

135M
Downloads

Our authors are among the

154
Countries delivered to

TOP 1%
most cited scientists

12.2%
Contributors from top 500 universities

WEB OF SCIENCE™

Selection of our books indexed in the Book Citation Index in Web of Science™ Core Collection (BKCI)

Interested in publishing with us?
Contact book.department@intechopen.com

Numbers displayed above are based on latest data collected.
For more information visit www.intechopen.com

12

Dynamic Analysis of an Automobile Lower Suspension Arm Using Experiment and Numerical Technique

S. Abdullah[1], N.A. Kadhim[1], A.K. Ariffin[1] and M. Hosseini[2]
[1]*Universiti Kebangsaan Malaysia*
[2]*Taylor's University College*
Malaysia

1. Introduction

All machines, vehicles and buildings are subjected to dynamic forces that cause vibration. Most practical noise and vibration problems are related to resonance phenomena where the operational forces excite one or more modes of vibration. Modes of vibration that lie within the frequency range of the operational dynamic forces always represent potential problems. Mode shapes are the dominant motion of a structure at each of its natural or resonant frequencies. Modes are an inherent property of a structure and do not depend on the forces acting on it. On the other hand, operational deflection shapes do show the effects of forces or loads, and may contain contributions due to several modes of vibration.

Modal analysis is an efficient tool for describing, understanding, and modelling structural dynamics (Sitton, 1997). The dynamic behaviour of a structure in a given frequency range can be modelled as a set of individual modes of vibration. The modal parameters that describe each mode are: natural frequency or resonance frequency, (modal) damping, and mode shape. The modal parameters of all the modes, within the frequency range of interest, represent a complete dynamic description of the structure. By using the modal parameters for the component, the model can subsequently be used to come up with possible solutions to individual problems (Agneni & Coppotelli, 2004).

Published studies have demonstrated the different purposes from performing modal analysis. Initially, Wamsler & Rose (2004) found the mode shapes and study the dynamic behavior of structure in automotive applications. Gibson (2003), presented a comparison of actual dynamic modal test data to the analytically predicted mode shapes and natural frequencies for a missile and its launcher structure that was created in MSC.Patran/MSC.Nastran. Then Guan et al. (2005) evaluated the modal parameters of a dynamic tire then carried out the dynamic responses of tire running over cleats with different speeds. In other study, Leclere et al. (2005) performed modal analysis on a finite element (FE) model of engine block and validated the experimental results. Hosseini et al. (2007) performed experimental modal analysis of crankshaft to validate the numerical results.

In particular, studies using a computational model to estimate component fatigue have been actively developed because of the low cost and time savings associated with the estimation (Yim & Lee, 1996; Lee et al., 2000; Kim et al., 2002; Jung et al., 2005). Recently, Choi et al.

(2007) used the damage index method to localize and estimate the severity of damage within a structure using a limited number of modal parameters for steel plate girder and other highway bridges. This article reports on experimental investigation on timber beams using experimental modal analysis to extract the required modal parameters. The results are then used to compute the damage index, and hence to detect the damage. By a studying the response of modal parameters, Damir (2007), investigated the capability of experimental modal analysis to characterize and quantify fatigue behaviour of materials. While, Jun et al. (2008) predicted the fatigue life at the design stage of the suspension system module for a truck and a flexible body dynamics analysis is used to evaluate the reliability of the suspension frame. Dynamic Stress Time History has been calculated using a flexible body dynamics analysis and the Modal Stress Recovery method through generating a FE model. Finally, Hosseini et al. (2009), utilized the frequency response analysis to obtain the transfer functions of a crankshaft. These transfer functions were used later to estimate the combustion forces of the engine.

In order to calculate the vibration fatigue damage from Power Spectral Density's (PSD's) of input loading and stress response, frequency response analysis was required. To perform this kind of analysis, an eigenvalue analysis was required to determine the frequencies to use as dynamic excitation. This can be accomplished automatically in a modal frequency or manually with a modal analysis. Once confidence was established in the frequency domain procedures, the global fatigue analysis could proceed. Numerical and experimental dynamic behaviour have been viewed as a result from FEA and test respectively. This was to identify the component resonance frequencies and to extract the damping ratios from experimental modal test which used in the numerical modal analysis for the FEA accuracy purposes. An experimental modal test is initiated and it has been compared with analytical simulation result for the purpose of validation. Initial static FEA has been performed as another kind of validation to get the model stress or strain distribution. Another purpose is to classify the suitable location for choosing the position of fixing the strain gauge in the experimental strain road data collection from the automobile lower suspension arm. The FEA and measured strain values have been compared. The FEA strain results showed acceptable agreement with the experimental strain road data collection.

2. Quasi-static atress analysis

The quasi-static analysis method is a linear elastic analysis that is associated with external load variations. The idea of this method is that each external load history acting on the component or structure is replacing by static unit load acting at the same location in the same direction as the history. A static stress analysis is then performed for each individual unit load. Dynamic stresses produced by each individual load history can be evaluated by multiplying that history by the static stress influences coefficients that result from the corresponding unit load. The principle of superposition is then used to calculate the total dynamic stress histories within the component. Eq. (1) represents the mathematical form of this method at a specific finite element node assuming plane stress considerations and linear elastic (Kuo & KelKar, 1995).

$$\sigma_x(t) = \sum_{i=1}^{n} \sigma_{xi} P_i(t)\ ;\ \ \sigma_y(t) = \sum_{i=1}^{n} \sigma_{yi} P_i(t);\ \ \tau_{xy}(t) = \sum_{i=1}^{n} \tau_{xyi} P_i(t) \tag{1}$$

where n is the number of applied load histories and $\sigma_{xi}(t)$, $\sigma_{yi}(t)$, $\tau_{xyi}(t)$ are the stress influence coefficients. A stress influence coefficient is defined as the stress field due to a unit load applied to the component at the identical location and in the same direction as the load history, $P_i(t)$.

The quasi-static method has routinely been used in the vehicle industry to ascertain stresses and fatigue life (Sanders & Tesar, 1978). They showed that the quasi-static stress-strain evaluation is a valid form of approximation for most industrial mechanisms that are stiff and operate subsequently below their natural frequencies. However, this is not true when the dynamics of the structure have significant influence on the fatigue life of the component. An overall system design is formulated by considering the dynamic environment. The natural frequencies and mode shapes of a structure provide enough information to make design decisions.

The Lanczos method (Lanczos, 1950), overcomes the limitation and combines the best features of the other methods. It requires that the mass matrix be positive semi-definite and the stiffness be symmetric. It does not miss roots of characteristic equation, but has the efficiency of the tracking methods; due to it only makes the calculations necessary to find the roots. This method computes accurate eigenvalues and eigenvectors. This method is the preferred method for most medium-to large-sized problems, since it has a performance advantage over the other methods. The basic Lanczos recurrence is a transformation process to tridiagonal form. However, the Lanczos algorithm truncates the tridiagonalization process and provides approximations to the eigenpairs (eigenvalues and eigenvectors) of the original matrix. The block representation increases performance in general and reliability on problems with multiple roots. The matrices used in the Lanczos method are specially selected to allow the best possible formulation of the Lanczos iteration.

3. Modal frequency response analysis

The frequency response analysis is used to calculate the response of a structure about steady state oscillatory excitation. The oscillatory loading is sinusoidal in nature. In its simplest case, the load is defined as having amplitude at a specific frequency. The steady-state oscillatory response occurs at the same frequency as the loading. The response can have time shift due to damping in the system. This shift in response is called a phase shift due to the peak loading and peak response no longer occurs at the same time Phase Shift, which is shown in Fig. 1.

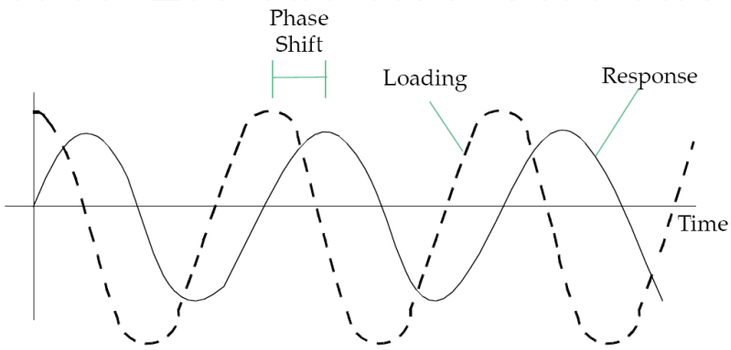

Fig. 1. Phase shift between loading and response amplitude

Modal frequency response analysis is an alternative approach to determining the frequency response of a structure. Modal frequency response analysis uses the mode shapes of the structure to reduce the size, uncouple the equation of motion (when modal or no damping is used), and make the numerical solution more efficient. Due to the mode shapes are typically computed as part of characterization of the structure, modal frequency response analysis is a natural extension of a normal mode analysis.

At the first step in the formulation, transform the variables from physical coordinates $\{u(\omega)\}$ to modal coordinates $\{\xi(\omega)\}$ by assuming

$$\{x\} = [\phi]\{\xi(\omega)\} e^{i\omega t} \tag{2}$$

The mode shapes $[\phi]$ are used to transform the problem in terms of the behaviour of the modes as opposed to the behaviour of the grid points. The Eq. (2) represents equality if all modes are used. However, due to all modes are rarely used, the equation usually represents an approximation.

Once, if all damping are ignored, the undamped equation for harmonic motion at forcing frequency ω is obtained in the form of the following equation:

$$-\omega^2 [M]\{x\} + [K]\{x\} = \{P(\omega)\} \tag{3}$$

Substituting the modal coordinate in Equation (2) for the physical coordinates in Eq. (3) and simplify, then the following is obtained:

$$-\omega^2 [M][\phi]\{\xi(\omega)\} + [K][\phi]\{\xi(\omega)\} = \{P(\omega)\} \tag{4}$$

The equation of motion using modal coordinates is finally obtained, but, the equation is still in the state of coupling. To uncouple the equation, pre-multiply both side of equation by $[\phi]^T$. Then, the new expression is presented in Eq. (5) as:

$$-\omega^2 [\phi]^T [M][\phi]\{\xi(\omega)\} + [\phi]^T [K][\phi]\{\xi(\omega)\} = [\phi]^T \{P(\omega)\} \tag{5}$$

where $[\phi]^T [M][\phi]$ is the generalized modal mass matrix, $[\phi]^T [K][\phi]$ is the generalized modal stiffness matrix, and $[\phi]^T \{P\}$ is the modal force vector.

The final step uses the orthogonal of the mode shapes to formulate the equation of motion in terms of the generalized mass and stiffness matrices, which are diagonal matrices. These diagonal matrices do not have the off-diagonal terms that couple the equation of motion. Therefore, in this form the modal equation of motion are uncoupled. In this uncoupled form, the equation of motion can be written as a set of uncoupled single degree-of-freedom systems as presented in Eq. (6), i.e.

$$-\omega^2 m_i \xi_i(\omega) + k_i \xi_i(\omega) = p_i(\omega) \tag{6}$$

where m_i is the i-th modal mass, k_i is the i-th modal stiffness, and p_i is the i-th modal force. If there is no damping has been included, the modal form of the frequency response equation of motion can be solved faster than the direct method, which it is due to an uncoupled single degree-of freedom system.

Vibration analysis (Crandell & Mark, 1973; Newland, 1993; Wirsching et al. 1995) is usually carried out to ensure that potentially catastrophic structural natural frequencies or resonance modes are not excited by the frequencies present in the applied load. Sometimes this is not possible and designers then have to estimate the maximum response at resonance caused by the loading.

4. Methodology

In order to achieve the objectives of the research, several steps in the flowchart, as presented in Fig. 2, should be implemented. In this flowchart, the three blocks; geometry, material, and loads and boundary conditions (loads and BCs) represent the input for the static and then modal frequency response finite element analysis, while only geometry and material represent the input for the numerical modal analysis. A comparison has been performed between the static analysis and road data strain results. If the strain result was almost the same in the critical area, then it can be considered as validation for the finite element analysis part. Then the model can be used in modal frequency response analysis. From another side, to identify the component resonance frequency and to extract damping ratios, which will be used later in the numerical modal analysis, experimental modal test has been performed. After that, another comparison has been performed between the experimental and numerical modal analysis, which can be considered as another validation for the finite element analysis part. The out put from the Modal frequency response analysis represents the most critical case result in a certain frequency which cause higher damage for the component if in reality it is work in this frequency. In a future work, this case result will be used as input for the fatigue analysis.

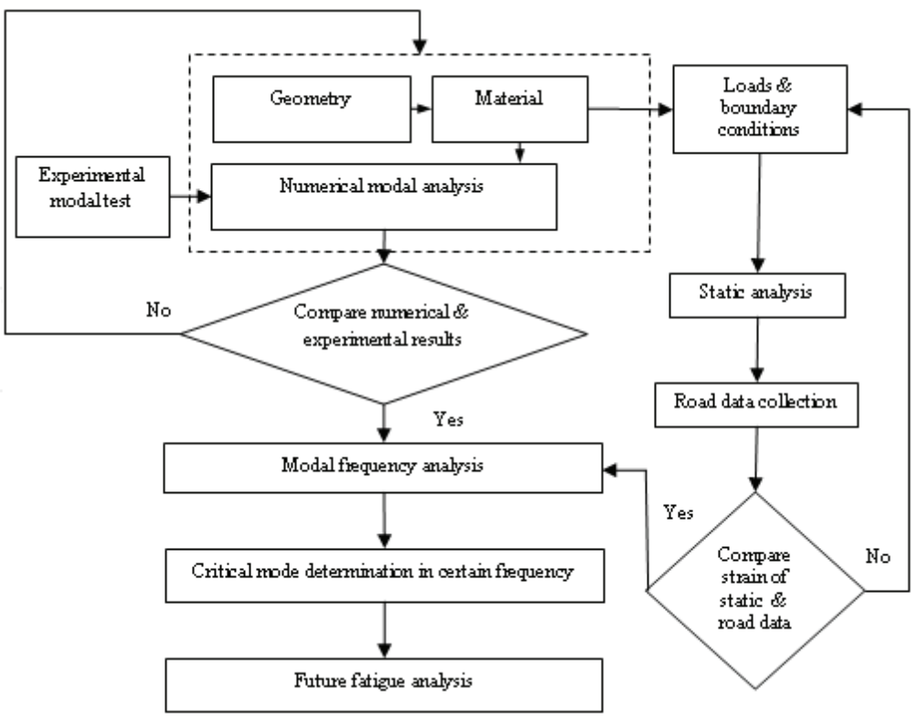

Fig. 2. Schematic diagram of research effort.

4.1 Geometry

A geometric model for an automobile lower suspension arm is considered in this study, and this component is presented in Fig. 3.

Fig. 3. A geometric model of an automobile lower suspension arm.

Three-dimensional lower suspension arm model geometry was drawn using the CATIA software, as shown in Fig. 4. The auto tetrahedral meshing approach is a highly automated technique for meshing solid regions of the geometry (MSC. Patran guide, 2002; Kadhim et al., 2010). It creates a mesh of tetrahedral elements for any closed solid including boundary representation solid. The tetrahedral meshing technique produces high quality meshing for boundary representation solids model imported from the most CAD systems. The specific mesh can give more accurate solution and the 10 nodes tetrahedral (TET10) element was used for the analysis with the adoption of a quadratic order interpolation function. A FE model of the lower suspension arm was implemented to find the modal parameters. According to 20 mm global edge element length, total of 25517 elements and 41031 nodes were generated for the model.

Fig. 4. An automobile lower suspension arm model.

4.2 Material

The purpose of analysing the chemical composition of a steel sample is to enable material classification. Based on Table 1, the steel sample can be classified as alloy steel since a carbon content range 0.27-0.33%, a manganese content range 1.4-2%, sulfur <= 0.04, silicon range 0.15-0.35% and phosphorous <= 0.035% (ASM specialty handbook, 1996). This represents the fabricated material for the 2000 cc Sedan lower suspension arm and was the material used in simulations. One sample was cut from the lower suspension arm using a cutter. The sample was subsequently ground with successive SiC papers (grit 200-1200) and then polished with polishing cloth and Alumina solution of grain size 6µm, and finally 1µm.

Element	C	Mn	Si	V	Cr	Ni	Pb	Fe
Measured value wt%	0.30	1.43	0.21	0.07	0.02	0.06	0.52	Balance

Table 1. Chemical composition of the steel

4.3 Normal modes analysis

Modal analysis is the process of determining modal parameters that are useful to understand the dynamic behaviour of the component. It may be accomplished either through analytical or experimental techniques (Hosseini et al., 2007), which are presented in the following parts.

4.3.1 Experimental

A schematic diagram of performing the experimental modal test is presented in Fig. 5. Measurements and recording of excitation and response signals were carried out over an automobile lower suspension arm.

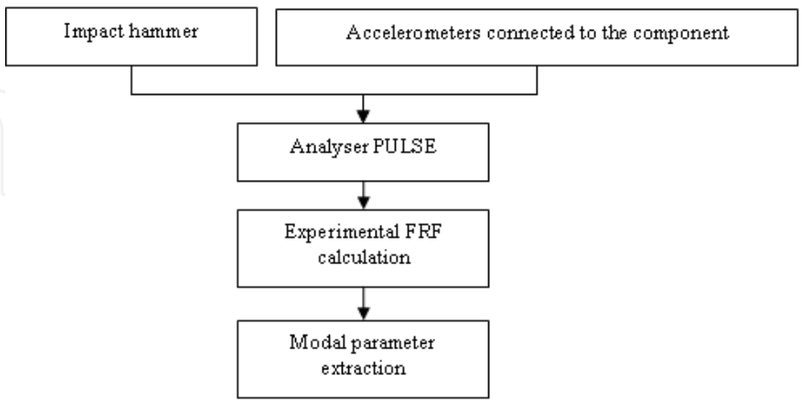

Fig. 5. Schematic diagram of experimental modal test

The component was impacted with a hammer along the x-axis as shown in Fig. 6, then another two measurements in y and z-axis separately. It was a SIMO system and the system response model can be written as follows:

$$\begin{bmatrix} y_1 \\ . \\ . \\ . \\ y_n \end{bmatrix}_{n\times 1} = \begin{bmatrix} H_1 \\ . \\ . \\ . \\ H_n \end{bmatrix}_{n\times 1} [F]_{1\times 1} \tag{7}$$

where n is the number of response channels along the object. Bruel & Kjaer portable and multi-channel analyzer PULSE type 3560D with ENDEVCO Isotron accelerometers type 751-100 and impact hammer type 2302-10 were utilized in the measurement devices. The Bruel & Kjaer Pulse LabShop was the measurements software and the B & K calibration exciter

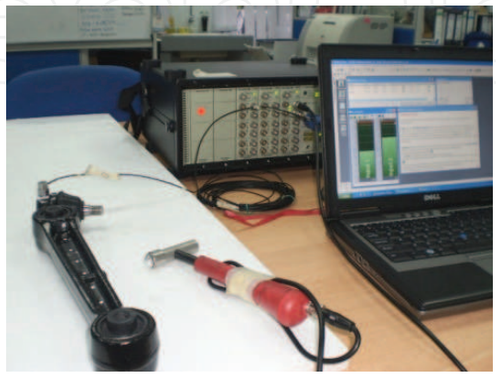

Fig. 6. The set up of data acquisition Portable Analyser Pulse to be used for normal mode analysis test

type 4294 was used to calibrate the accelerometer. In order to approximate free condition, lower suspension arm was placed on a soft Styrofoam. The uni-axial accelerometer was attached first alongside x direction then y and z-direction. In the single input experiment, the lower suspension arm was impacted with one hammer along the x, y, then z-axis separately. It was single input-multiple output system.

Three equipment functions should be considered in the process of experimental modal testing (Cantley, 2003): Excitation method, response measurement method, Data acquisition, and analysis software.

Modal damping was measured automatically by the analyzer PULSE at each resonance through identifying the half power (-3 db) points of the magnitude of the frequency response function. For a particular mode, damping ratio ζr is calculated by

$$\varsigma_r = \frac{\Delta f}{2 f_r} \tag{8}$$

where Δf is the frequency band width between the two half power points and f_r is the resonance frequency. PULSE type 3560 contains a built-in standard cursor reading, which calculates the modal damping. The accuracy of this method is dependent on the frequency resolution (1 Hz for this measurement) used for the measurement because this determines show accurately on the computer screen the peak magnitude can be measured.

The weight of the accelerometer was 7.8 g. The weight of the lower suspension arm was 2.4 kg, which was made of SAE1045 steel, and despite the size, it was much heavier than the accelerometer. The total weight of the accelerometers was 0.3% of the lower suspension arm and had negligible effects on the measurement.

4.3.2 Analytical

In numerical method, a FE model of the component was created by MSc.Patran and sent to MSc.Nastran for analysis. The output transferred back to MSc.Patran for visualization of the results. Damping was measured during the experimental part and updated into the numerical analysis. These values only have meaning around resonance frequencies; mass and stiffness components neutralized each other and damping could be calculated. Lumped mass characteristic was used for modelling the structure to save memory and time needed for analysis. The Lanczos method was utilized to extract eigenvalues for all the modes of such a medium model in the frequency span of 5 kHz. It substantially increases computational speed and reduces disk space. The main advantages of finite element models are:4 models used for design development and no prototypes are necessary, while the disadvantages are: modelling assumptions, joint design difficult to model, component interactions are difficult to predict and damping generally ignored.

4.4 Loads and boundary conditions

Three main parts in the lower suspension arm has been considered in the FE boundary conditions, i.e. ball joint, bushing_1 and bushing_2. Fig. 7 shows the FE model with related boundary conditions applied at specific location.

In the analysis, a distributed load has been applied on the inner surface of bushing_1. Bushing_2 considers as a rigid section with a rotation around x-axis from the side of the vehicle body. In the same time, the rigid condition has been considered on the ball joint with

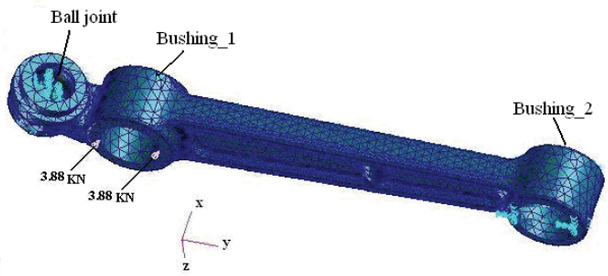

Fig. 7. Finite element model of the lower suspension arm

translations in x and y direction while the rotation around x, y, and z-axis is used to represent the braking and cornering loads. There are no acceleration loads as inputs for the analysis, due to collecting data during driving of the car at constant sped.

4.5 Static analysis

An initial static FEA has been performed to obtain the strain distribution along the lower suspension arm, in order to classify the critical areas for choosing the position of fixing the strain gauges during the strain data collection, which explained in next section. After that, the measured values of strain were used later for validation purposes of the applied load values and boundary conditions in the static and frequency FEA through the measured strain values and experimental identification for the higher stress or strain area of the component as damage criteria.

4.6 Road data collection

A distribution load has been applied on the inner surface of bushing_1 with a value of 3.88 kN with a slope of 60° as a result for load calculation which effected on the lower arm due to vehicle and passengers weight. To ensure the reliability and for validation purposes, a load history was obtained from the real automotive lower suspension arm of this study, which was driven over a country road. The frequency sample, fs, for this case was 500 Hz. This f_s value was chosen in order to improve the accuracy of the data (Stephens et al., 1997; Oh, 2001). The data was measured using a data acquisition system at an automobile speed of 25 km/h, and recorded as strain time histories. The data acquisition set-up is shown in Fig. 8.

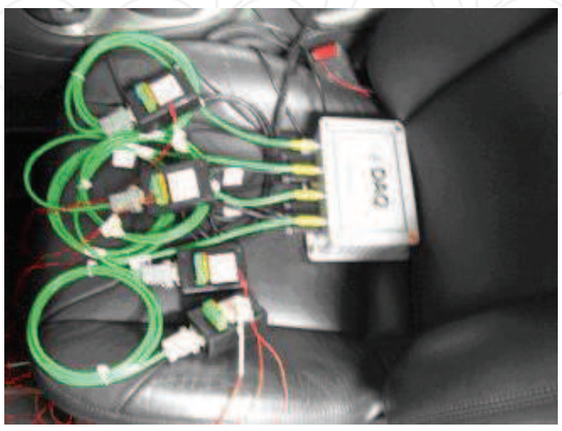

Fig. 8. The set up of data acquisition used for data collection

The strain gauge could not be physically fixed at the most critical point due to its design. Four strain gauges were fixed at different locations, as shown in Fig. 9. After collecting the data for four strain gauges for the country road type at different locations (Fig. 10) and for the confirmation purposes of the current FEA reliability, the damage was determined for all the collected load histories (Table 2) by using a software as explained in the schematic diagram in Fig. 11.

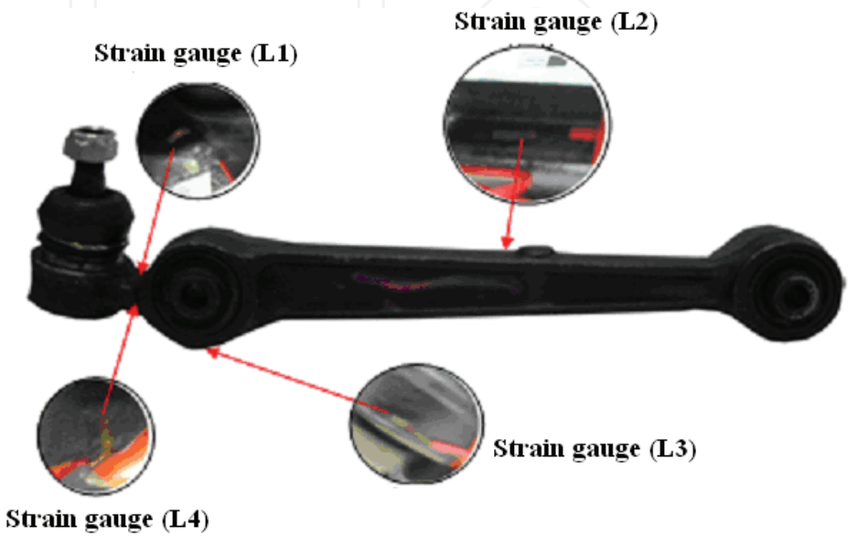

Fig. 9. The strain gauge positions on the lower suspension arm

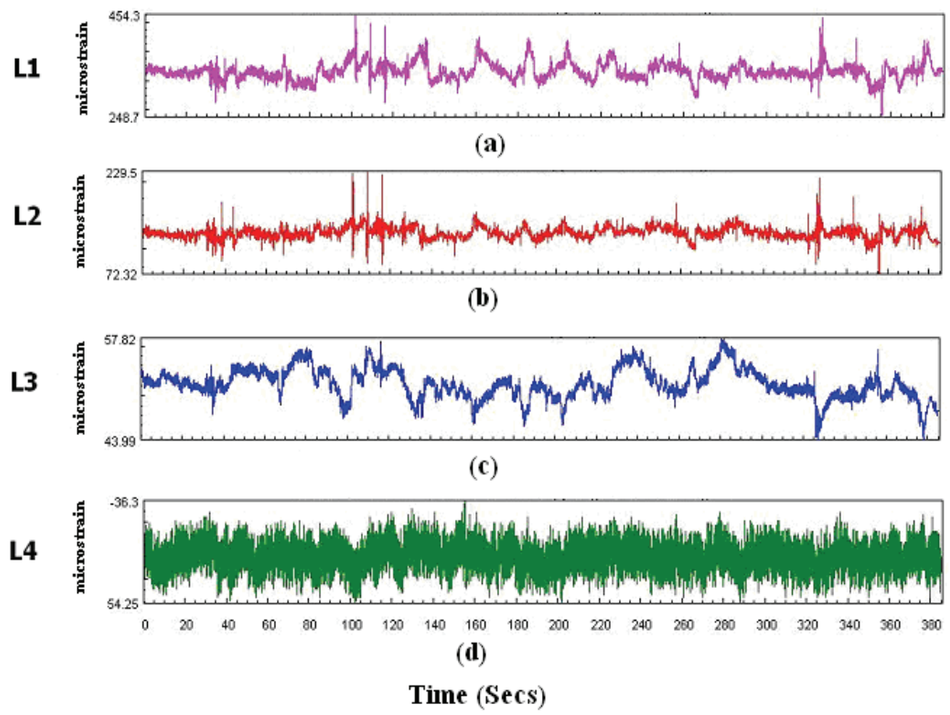

Fig. 10. Strain time history plot for different strain gauge positions: (a) L1, (b) L2, (c) L3, (d) L4

Strain gauge signal	Damage
L1	0.734
L2	0.0888
L3	0.0033
L4	4.8E-6

Table 2. The fatigue damage values for different strain loadings

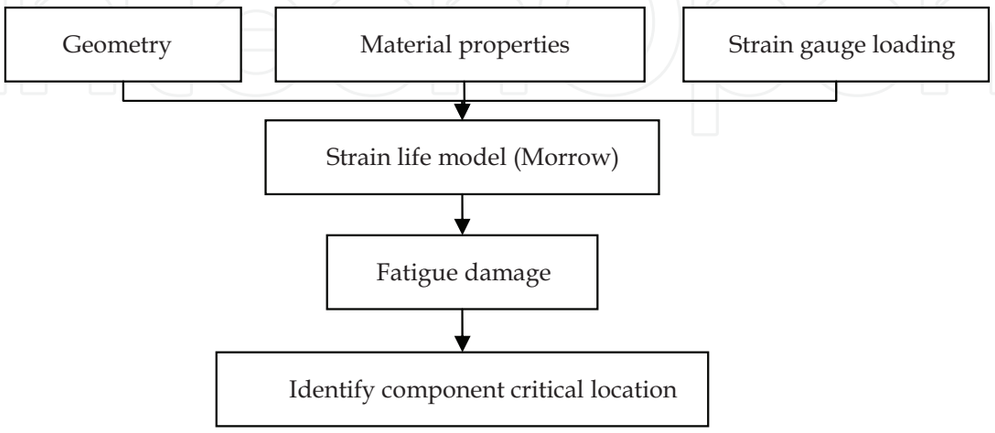

Fig. 11. Schematic diagram of calculating fatigue damage values for the collected loadings

The life has been calculated using Morrow strain life model. Based on the model developed by Morrow (1968), the relationship of the total strain amplitude (ε_a) and the fatigue life in reversals to failure (2Nf) can be expressed as

$$\varepsilon_a = \frac{\sigma'_f}{E}\left(1-\frac{\sigma_m}{\sigma'_f}\right)\left(2N_f\right)^b + \varepsilon'_f\left(2N_f\right)^c \tag{9}$$

where E is the material modulus of elasticity, ε_a is the true strain amplitude, $2N_f$ is the number of reversals to failure, σ'_f is the fatigue strength coefficient, b is the fatigue strength exponent, ε'_f is the fatigue ductility coefficient and c is the fatigue ductility exponent, σ_m is the mean stress.

The damage fraction, D, is defined as the fraction of life used up by an event or a series of events. Awareness of these individual cycles' lives, however, still does not immediately indicate the predicted life and reliability for an actual variable amplitude history. To obtain the life of a whole loading history block, a damage summation model will attempt to combine the individual life found for each defined cycle into the predicted reliability for the whole history. With respect to the relationship between damage and cycle, the damage for one cycle, D_i , can be calculated as

$$\text{Di} = 1/\ \text{N}_\text{f} \tag{10}$$

where N_{fi} is the number of constant amplitude cycles to failure. To calculate the fatigue damage for a block of VA loading, a linear cumulative damage approach has been defined by Palmgren (1924) and Miner (1945). The technique, known as the Palmgren-Miner (PM) linear damage rule, is defined as

$$D = \sum_{i=1}^{n} \frac{N_i}{N_{fi}} = 1 \tag{11}$$

where n is the number of loading blocks, N_i is the number of applied cycles and N_{fi} is the number of constant amplitude cycles to failure. The failure will occur when the summation of individual damage values caused by each cycle reaches a value of one. After the fatigue damage for a representative segment or block of load history has been determined, the fatigue life for each block is calculated by taking the reciprocal.

4.7 Modal frequency response analysis

Frequency based FEA can be a powerful qualitative as well as quantitative tool for reliability assessment of certain components. One of the main capabilities for the fatigue analysis of dynamic system is a vibration fatigue analysis, which requires input PSDs, and cross PSDs, and the structure transfer functions computed by FE model. Once these transfer functions are available, any number of duty cycles can be accommodated with some computational effort. The frequency response analyses were performed using the procedure explained in Fig. 2. The 3.88 KN load applied with arrange of frequency between 500 Hz and 5000 Hz which can give changing in load value during the analysis. Frequency response analysis with damping was implemented. The extracted damping ratio from experimental modal test had been used in modal frequency response analysis. It is the ratio of the actual damping in the system to the critical damping. Most of the experimental modal reported that the modal damping in terms of non-dimensional critical damping ratio expressed as a percentage (Formenti, 1999; Gade et al., 2002). In fact, most structures have critical damping values in the range of 0 to 10%. Zero damping ratio indicates that the mode is undamped. Damping ratio of one represents the critically damped mode.

5. Results and discussions

The modal analysis is usually used to determine the natural frequency, damping and mode shape parameters of a component. The dynamic characteristics such as natural frequency and mode shape can be obtained experimentally and predicted analytically while the damping ratio can be measured only experimentally. It can be used as the starting point for the frequency response, the transient and random vibration analyses. The extracted number of modes was useful to understand the dynamic behaviour of the component such as the natural frequency span and the extracted damping ratio from the experimental which used in the numerical analysis. The frequency response analysis (FRF) output can be considered as the most important input for the future vibration fatigue analysis.

A sampling rate of 5000 Hz was used in order to capture the whole vibration characteristics (Aykan & Celik, 2009). Based on the obtained data from the modal analysis simulation (Table 3), frequency up to 5000 Hz, can give six modes starting from 1172 and end in 4578 Hz. This is true since the modes or resonances are inherent properties of the structure (Bujang et al., 2008). In theory, resonance is determined by the material properties and the boundary conditions of the component (Alfano et al., 2008). Therefore, if the material properties of the component change, the modes will change. The mode shape results with their frequencies for the first three modes of an automobile lower suspension arm are shown in Fig. 12 as the mode shape deflection pattern is clearly shown. These results can be useful for designers to understand the dynamic characteristics of the component in order to take a decision to build their design depending on the mode number, which can provide higher

stress to represents the most critical mode. According to the boundary conditions and material properties, the deflection of the component can be noticed in the y-z plane. Mode 1 is bending in y-z, mode 2 is twisting in y-z, and mode 3 is sine shape in y-z.

Mode no.	Natural Frequency (Hz)
1	1172
2	1560
3	2809
4	3159
5	4175
6	4578

Table 3. The natural frequency results obtained from modal analysis

Mode 1, 1560 Hz Mode 2, 3159 Hz Mode 3, 4175 Hz

Fig. 12. Simulated modal frequencies and mode shapes from FEA

The frequency response analysis was performed experimentally and analytically using the particular FEA code. It used the damping ratio that extracted from the experimental modal test. The output result file for this type of analysis represented by the stress values for the most damaging mode were used as one of the main input for vibration fatigue analysis. Four natural frequencies were detected from the modal test in 537, 1738, 3394, and 4360 Hz as shown in Fig.13.

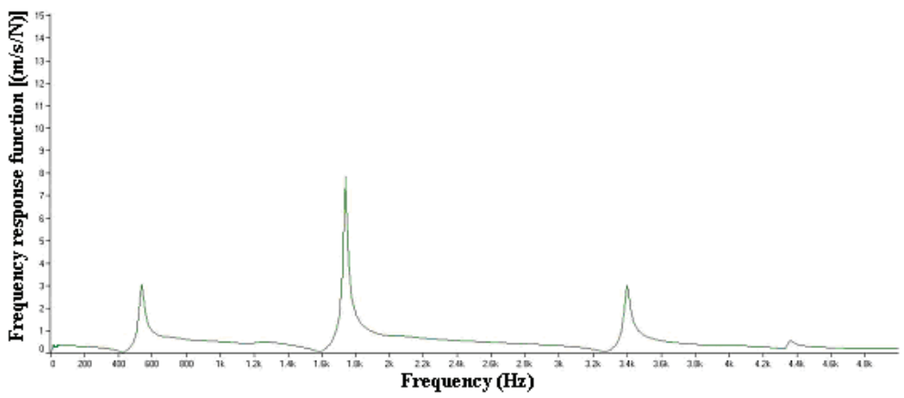

Fig. 13. Automobile lower suspension arm FRF plotted against frequency (0-5000 Hz)

The experimental results represented by the natural frequency with its damping ratio are shown in Table 4. The damping ratio is the ratio of the actual damping in the system to the critical damping. In fact, most structures have critical damping values in the range of 0 to

10%, with values of 1 to 5% as the typical range (Dynamic analysis user's manual, 2005). A zero damping ratio indicates the mode is undamped.

No.	Experimental Natural Frequency (Hz)	Experimental damping ratio (%)
1	537	2.19
2	1738	0.89
3	3394	0.47
4	4360	0.9

Table 4. The experimental natural frequency and damping ratio

The extracted damping ratio from the experimental modal test has been feed back to the numerical modal analysis to increase the analysis accuracy. There are some differences in the resonance or natural frequency between the numerical and the experimental. This is due to consider the standard material properties for the SAE 1330H steel in the modal analysis, which did not represent the lower suspension arm fabricated SAE 1330H steel properties. The material properties of the fabricated lower suspension arm are different from the standard (ASM Specialty Handbook, 1996). This is due to the elements addition by the manufactured company to improve the component performance. Only one kind of experiment has been performed to specify one of the fabricated material properties represented by the density measurement, which has the value of 7.75 g/cm3. The density has been measured using Electronic Densitimeter (MD-200S) and used as input for the FEA.
The first and third experiment natural frequencies (Fig.13) could not be detected by FEA while second and fourth were detected. The first natural frequency from the FEA represents the most important stress result due to consider it as the most critical frequency in the experimental and analytical work and its FEA stress results was used later in vibration fatiue analysis. These differences were due to manipulation error as a possible source of error (Robert et al., 2002) which is introduced as equations are processed; for example, results of multiplication are truncated or rounded. Manipulation error may be minor if global equations [k]{D}={R} are solved once, as in time-independent analysis. In some dynamic and nonlinear problems, where each step builds on the step before and a calculation sequence must be executed repeatedly, manipulation error may accumulate. Another source may be due to not using the exact material properties as mentioned before
The result of the frequency response analysis with zero Hz is presented in Fig.14 for AISI 1330H_steel. It can be noticed that the maximum principal stress is 271 MPa at zero Hz. The variation of the maximum principal stresses with the frequency range 0-5000 Hz is shown in Fig.15. It is observed that the maximum principal stress occurs at a frequency of 1560 Hz for the first mode with value of 865 MPa. This value of stress is for the most critical case in the frequency response analysis and it is also shown as contour graph in Fig.16. This value is less than the tensile yield stress value of 1034 MPa for the AISI 1330H steel. It also can be noticed that the maximum principal stresses varies with the frequencies. This variation is due to the dynamic influences of the first mode shape.
From the results and analysis obtained in this research, it is noticed that modal and frequency response analysis is an efficient tools to understand the dynamic behaviour of the component. This type of analysis can provide information about the modal parameters and

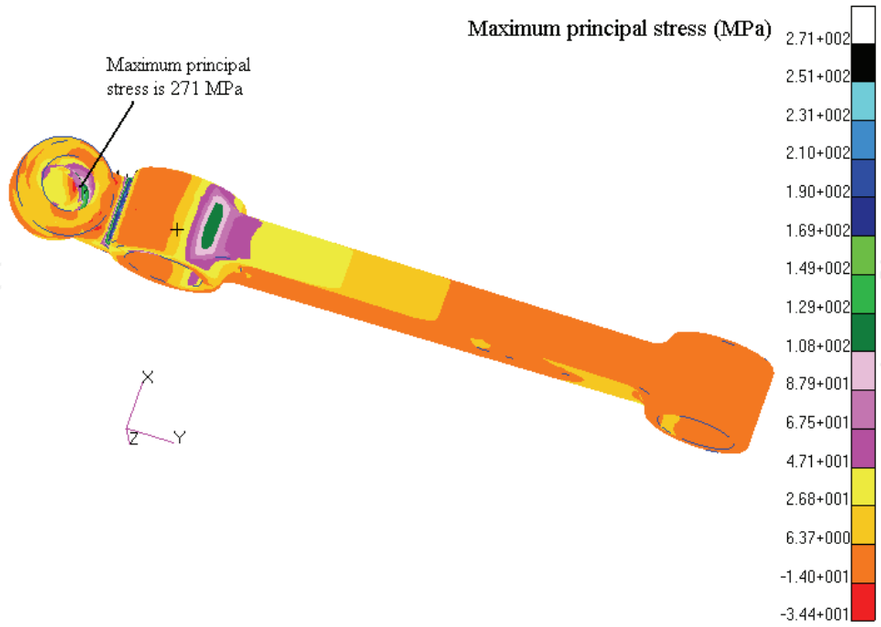

Fig. 14. The Maximum principal stress distribution for the frequency response analysis with zero Hz for AISI 1330H_steel

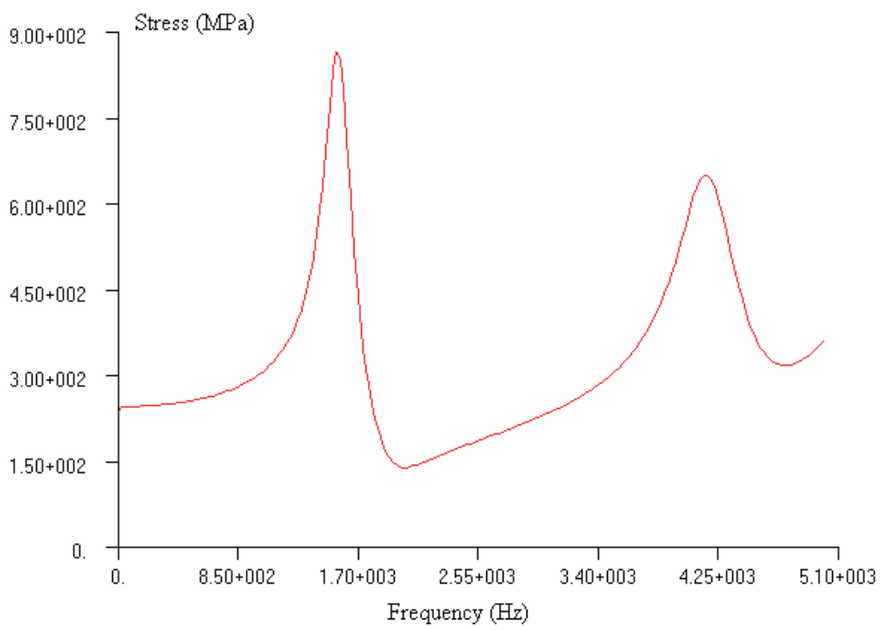

Fig. 15. Automobile lower suspension arm stress plotted against frequency (0-5000 Hz)

the stress distribution to be used to predict fatigue life in vibration analysis. For further validation purposes, static analysis has been performed and its result has been compared with the road strain data. Finally, it is suggested to perform the vibration fatigue analysis depending on the frequency response analysis result in automotive durability research for the purpose of component life estimation under random loading.

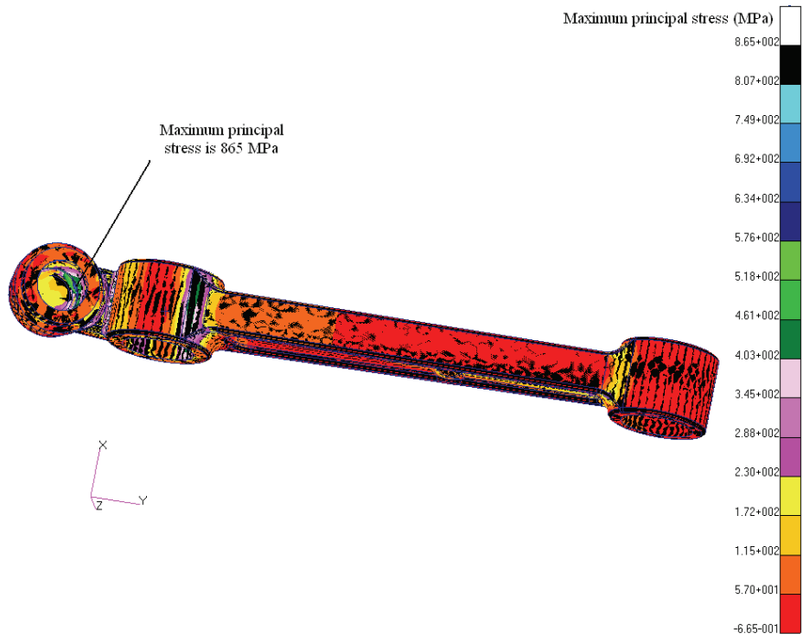

Fig. 16. The maximum principal stress contour for the frequency response analysis at 1560 Hz

6. Conclusion

The research was carried out to investigate the dynamic characteristic of the automotive lower suspension arm, experimentally and numerically. FEA part as a numerical technique has been validated. Another validation has been performed through a comparison of the static FEA predicted strain data and experimentally collected road strain data. One of the most important parts of a vibration fatigue analysis is the calculation of transfer functions. With NASTRAN this is called a frequency response analysis, so this kind of analysis has been performed for future vibration fatigue analysis.

One of the results expected to show higher stress effects on the component in a certain frequency. In another words, it was to extract the FRF of the component in most critical vibration mode in order to use it as a specific resonance in vibration fatigue analysis, which can be examined, then solved for the purpose of component life estimation. The mode 1 of 1172 Hz has been found as the most critical mode. Both of the maximum principal strain contours plots are identical for static and frequency response analysis at zero Hz. This result is a proof that strain distribution of the lower suspension arm has been reliably predicted using the finite element model. This study has highlighted the need for experimental work to validate FEA modelling and to allow its advantages be maximised. Work is currently under progress to exploit this research results to investigate the lower suspension arm vibration fatigue life and to perform optimization studies to assess how to overcome various dynamic problems.

7. Acknowledgment

The authors would like to express their gratitude to University Kebangsaan Malaysia and Ministry of Science, Technology and Innovation, through the fund of 03-01-02-SF0052, for supporting these research activities.

8. References

Agneni, A. & Coppotelli, G. (2004). Modal parameter prediction for structures with resistive loaded piezoelectric devices. *Experimental Mechanics*, Vol. 44, No.1, 2004, pp. 97-100, ISSN. 10.1007/BF02427983.

Alfano, M., Pagnotta, L., Stigliano, G. (2008). Elastic properties of cold rolled aluminium plates with irregular shape by dynamic testing. *International conference on engineering optimization,* pp. 01 – 05, Rio de Janeiro, June 2008, Brazil

ASM Specialty Handbook. (1996). *Carbon and Alloy Steels*, edited by J. R. Davis & Associates, ASM International, Metals Park, OH, Metals Handbook, Vol. 1 – properties and Selection: irons, Steels, and High-Performance Alloys, ASM International 10th Ed.1990)

Aykan, M.& Celik, M. (2009). Vibration fatigue analysis and multi-axial effect in testing of aerospace structures. *Mechanical Systems and Signal Processing*, Vol. 23, pp. 897–907, 0888-3270

Bujang, I. Z., Kamaruddin, K. A. & Nordin, M. T. (2008). Identification of Structural Defects Using Modal Technology. *International conference on constucyion and building technology*. Malaysia

Cantley, C. (2003). Modal testing facility for advanced LIGO, University of Glasgow, *Advanced LIGO SUS Workshop*, LIGO-G030534-00-K

Choi, F. C.; Li J. & Samali B. (2007). Application of modal-based damage-detection method to locate and evaluate damage in timber beams, *J. Wood Science* 53(5) 394-400.

Crandell, S.H. & Mark W.D. (1973). *Random vibration in mechanical systems*, Academic Press, 0121967506, New York

Damir, A.N.; Elkhatib A. & Nassef G. (2007). Prediction of fatigue life using modal analysis for grey and ductile cast iron, *International J. Fatigue*, Vol. 29, pp. 499-507, 0142-1123

Formenti, D. (1999). The relationship between % of critical and actual damping in a structure, *J. Sound & Vibrations*, Vol. 33, No. 4, pp. 14-18, 0022-460X

Gade, S; Herlufsen, H. & Konstantin-Hansen H. (2002). How to determine the modal parameters of simple structures. *J. Sound & Vibrations,* Vol. 36, No. 1, pp. 72-73, 0022-460X

Gibson, M.E. (2003). Correlation of modal results from a MSC.Patran/MSC.Nastran finite element model to modal test, Presented at the *Virtual Product Development Conference*, pp. 1-22, Dearborn, April 2003, Michigan.

Guan, D.; Fan C. & Xie X. (2005). A dynamic tyre model of vertical performance rolling over cleats, *J. Vehicle System Dynamics*, Vol. 43, No. 1, 2005, pp. 209-222, 10.1080/00423110500109398

Hosseini, M.; Mohd M.; Ariffin A. & Abdullah S. (2009). Inverse combustion force estimation based on response measurements outside the combustion chamber and signal processing, *Mech. System and Signal Processing*, Vol. 23, pp. 2519-2537

Hosseini, M.; Mohd, M.; Ariffin, A. & Abdullah, S. (2007). Mobility analysis of vehicle crankshaft, in Proc. *Conference on Advances in Noise, Vibration and Comfort*, pp. 167-175*,* Selangor, Malaysia, November 2007, Putrajaya.

Jun, K. J., Park T.W., Lee S. H., Jung S.P. & Yoon J.W. (2008). Prediction of fatigue life and estimation of its reliability on the parts of an air suspension system, *International J. Automotive Technology*, Vol. 9, No. 6, pp. 741−747, 1976-3832

Jung, H.; Park, T. W.; Seo, J. H.; Jun, K. J.; Yim, H. J.; Kim, H. & Park, J. K. (2005). A study on the fatigue life prediction of OHT vehicle structures using the modal stress recovery method. *Proc. IDETC/CIE*, DETC 2005-84319.

Kadhim, N.A.; Abdullah, S. ; Ariffin, A.K. & Beden, S.M. (2010). Fatigue behaviour of automotive lower suspension arm, 8th International conference on fracture and stength of solids (FEOFS 2010), pp. 1-6, Istana hotel, June 2010, Kuala Lumpur

Kim, H.S.; Yim, H.J. & Kim, C.M. (2002). Computational durability prediction of body structure in prototypes vehicles. *International J. Automotive Technology*, Vol. 3, No. 4, pp 129-136, 1976-3832

Kuo, E.Y. & Kelkar S.G. (1995). Body structure durability analysis, *Automotive Eng*. Vol. 103, No. 7, pp. 73-77, 0098-2571

Lanczos, C. (1950). An iteration method for the solution of the eigenvalue problem of linear differential and integral operators, *J. Research of the National Bureau of Standards* Vol. 45, No. 4, pp. 255-282, 0091-0635, OCLC: 4723507

Leclere, Q.; Pezerat C.; Laulagnet B. & Polac L. (2005). Indirect measurement of main bearing loads in an operating diesel engine. *J. Sound and Vib*ration, Vol. 286, No. 1-2, August 2005, pp. 341–361, 0022-460X

Lee, S. B.; Park, T. W. & Yim, H. J. (2000). A study on computational method for fatigue life prediction of vehicle structure, *J. KSNVE*, Vol. 10, No. 4, pp. 686-691, 0963-8695

Miner, M. A. (1945). Cumulative damage in fatigue, *J. Appl. Mech*., Vol. 67, pp. A159-A164, 0021-8936

Morrow, J. (1968). *Fatigue Design Handbook*, Advances in Eng., Society of Automotive Engineers, Warrendale, Pa., Vol. 4, pp. 3-36, 978-1-56091-917-9

MSC. NASTRAN. (2005). *MSC. NASTRAN dynamic analysis user's manual*. Los Angles, USA: MSC Software Corporation

MSC. Patran users guide (2002). Vol.1. Los Angles, MSC. Software Corporation. USA

Newland, D.E. (1993). *An introduction to random vibrations, spectral and wavelet analysis*, (Essex, Longman Scientific and Technical)

Oh, C.S. (2001). Application of wavelet transform in fatigue history editing, *International J Fatigue*, Vol. 23, No. 3, pp. 241-250, 0142-1123

Palmgren. (1924). Die Lebensdauer von Kugellagern, *Verfahrenstechinik*, Berlin, Vol. 68, pp. 339-341

Robert, D.; David S.; Michael E. & Robert J. (2002). *Concepts and applications of finite element analysis*. USA, John Wiley and Sons

Sanders, J.R. & D. (1978). Tesar, The analytical and experimental evaluation of vibration oscillations in realistically proportioned mechanisms. *ASME Paper* No. 78-DE-1

Sitton, G. (1997). *MSC/NASTRAN Basic dynamic analysis-user's guide*, Vol. 1, The MacNeal-Schwendler Corporation, USA.

Stephens, R.I.; Dindinger P.M. & Gunger J.E. (1997). Fatigue damage editing for accelerated durability testing using strain range and SWT parameter criteria, *International J. Fatigue*, Vol. 19, No. 8-9, pp. 599-606, 0142-1123

Wamsler, M. & Rose, T. (1998). Advanced mode shape identification method for automotive application via modal kinetic energy plots assisted by numerous printed outputs. Presented at the *MSC Americas Users' Conference*, pp. 1-17, Sheraton Universal Hotel, Universal City, October 1998, California.

Wirsching, P.H.; Paez, T.L. & Oritz, K. (1995). *Random vibration: theory and practice*, John Wiley and Sons, Inc., 0-471-58579-3, New York

Yim, H.J. & Lee, S.B. (1996). An integrated CAE system for dynamic stress and fatigue life prediction of mechanical systems, KSME International J., Vol. 10, No. 2, pp. 158-168, 1226-4865

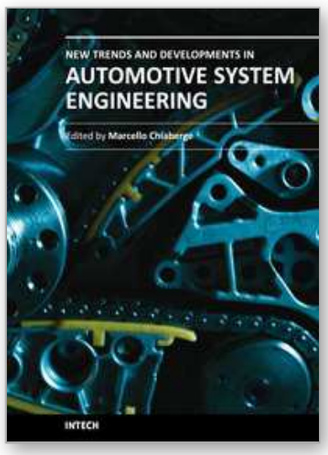

New Trends and Developments in Automotive System Engineering
Edited by Prof. Marcello Chiaberge

ISBN 978-953-307-517-4
Hard cover, 664 pages
Publisher InTech
Published online 08, January, 2011
Published in print edition January, 2011

In the last few years the automobile design process is required to become more responsible and responsibly related to environmental needs. Basing the automotive design not only on the appearance, the visual appearance of the vehicle needs to be thought together and deeply integrated with the â€œpowerâ€ developed by the engine. The purpose of this book is to try to present the new technologies development scenario, and not to give any indication about the direction that should be given to the research in this complex and multi-disciplinary challenging field.

How to reference
In order to correctly reference this scholarly work, feel free to copy and paste the following:

S. Abdullah, N.A. Kadhim, A.K. Ariffin and M. Hosseini (2011). Dynamic Analysis of an Automobile Lower Suspension Arm Using Experiment and Numerical Technique, New Trends and Developments in Automotive System Engineering, Prof. Marcello Chiaberge (Ed.), ISBN: 978-953-307-517-4, InTech, Available from: http://www.intechopen.com/books/new-trends-and-developments-in-automotive-system-engineering/dynamic-analysis-of-an-automobile-lower-suspension-arm-using-experiment-and-numerical-technique

INTECH
open science | open minds

InTech Europe
University Campus STeP Ri
Slavka Krautzeka 83/A
51000 Rijeka, Croatia
Phone: +385 (51) 770 447
Fax: +385 (51) 686 166
www.intechopen.com

InTech China
Unit 405, Office Block, Hotel Equatorial Shanghai
No.65, Yan An Road (West), Shanghai, 200040, China
中国上海市延安西路65号上海国际贵都大饭店办公楼405单元
Phone: +86-21-62489820
Fax: +86-21-62489821

© 2011 The Author(s). Licensee IntechOpen. This chapter is distributed under the terms of the Creative Commons Attribution-NonCommercial-ShareAlike-3.0 License, which permits use, distribution and reproduction for non-commercial purposes, provided the original is properly cited and derivative works building on this content are distributed under the same license.

IntechOpen

IntechOpen